11th World Congress on Computational Mechanics (WCCM XI)
5th European Conference on Computational Mechanics (ECCM V)
6th European Conference on Computational Fluid Dynamics (ECFD VI)
E. Oñate, J. Oliver and A. Huerta (Eds)

VISCOPLASTIC REGULARIZATION OF STRAIN LOCALIZATION IN FLUID-SATURATED POROUS MEDIA

MARIA LAZARI, LORENZO SANAVIA AND BERNHARD A. SCHREFLER

Department of Civil, Environmental and Architectural Engineering,
University of Padova
via Marzolo 9, 15131 Padova, Italy
e-mail: maria.lazari@unipd.it, lorenzo.sanavia@unipd.it, bernhard.schrefler@dicea.unipd.it,
www.dicea.unipd.it

Key Words: *Strain Localization, Viscoplastic Regularization, Multiphase Porous Materials, Quasi-static loading, Drucker-Prager.*

Abstract. In this paper, viscoplasticity is adopted as regularization technique to avoid the mesh sensitivity problem in strain localization simulation of multiphase geomaterials in quasi-static and isothermal conditions. Drucker-Prager yield surface with isotropic linear hardening/softening and non-associated plastic flow is used for simplicity. The regularizing effect of viscoplastic model is analyzed by numerical simulation of an undrained plane strain biaxial compression test on initially water saturated dense sand. Mesh sensitivity is examined by using different spatial discretization and the results denote the crucial influence of the loading velocity on the viscous regularization of quasi-static process.

1 INTRODUCTION

Strain softening in geomaterials is usually accompanied by localized deformation and lead to ill-posedness of the boundary value problem when a Cauchy continuum is used. Mathematically, it has been widely recognized that the governing differential equations loose ellipticity and become ill-posed at the onset of localization, as a consequence of material instability. The boundary value problem may exhibit an infinite number of linearly independent solutions or the solutions of the boundary value problem do not depend continuously on the data [1]. From the numerical point of view, ill-posedness is manifested by excessive pathological sensitivity of the results to the size of finite elements.

In the framework of single phase solids, several techniques for regularizing the quasi-static (or dynamic), boundary (or initial) value problem with material instability can be found in the literature [2,3,14,18,19,21,28]. In case of multiphase porous media, strain localization problems have been studied the recent years, using rate-dependent constitutive models [5,16,25,27], gradient plasticity models [29] or by using a micropolar continuum [6].

Aiming at geotechnical applications, the coupling of the solid deformation with the pore-fluid flows is of great importance and should not be neglected. The objective of the present paper is to simulate strain localization of multiphase materials without mesh dependency. Herein, viscoplasticity is adopted as regularization technique in the post bifurcation regime. More specifically, a local viscoplastic constitutive model of Perzyna type and its consistent viscoplastic tangent operator have been formulated and implemented in the finite element code Comes-geo [7,8,9,15,23,24] developed at the University of Padua based on the multiphase porous media model developed in [15]. The effectiveness of the model is examined by the simulation of a biaxial compression test. The results indicate that rate dependency prevents strains from localizing into infinitely narrow bands when the mesh is refined.

2 MATHEMATICAL MODEL

The full mathematical model necessary to simulate the thermo-hydro-mechanical transient behaviour of variably saturated porous media has been developed within the Hybrid Mixture Theory in [15,26] following [10,11,12,13].

The variably saturated porous medium is treated as a multiphase system composed of solid skeleton (*s*) with open pores filled with liquid water (*w*) and gas (*g*). The latter, is assumed to behave as an ideal mixture of dry air (non-condensable gas, *ga*) and water vapour (condensable one, *gw*). The solid is deformable and non-polar and the fluids, solid and thermal effects are coupled. All fluids are in contact with the solid face. In the model, heat conduction and heat convection, vapour diffusion, (liquid) water flow due to pressure gradients or capillary effects and water phase change (evaporation and condensation) inside the pores are taken into account.

In the partially saturated zones the liquid water is separated from its vapour by a concave meniscus (capillary water). Due to the curvature of this meniscus, the sorption equilibrium equation [10] gives the relationship $p^c=p^g-p^w$ between the capillary pressure $p^c(\boldsymbol{x},t)$ (also known as matrix suction), gas pressure $p^g(\boldsymbol{x},t)$ and water pressure $p^w(\boldsymbol{x},t)$ where, $\boldsymbol{x}$ is the vector of the spatial coordinates and t the current time. Note that pore pressure is defined as compressive positive for the fluids, while stress is defined as tension positive for the solid phase.

The state of the medium is described by gas pressure p^g, capillary pressure p^c, temperature T and displacements of the solid matrix $\boldsymbol{u}$. The balance equations were developed in geometrically linear framework and are written here at the macroscopic level considering quasi-static loading conditions.

For the sake of completeness the model is only briefly summarized in this section and more details can be found in [23]. In what follows symbols in bold indicate vectors or tensors.

2.1 Equilibrium equation

The equilibrium equation of the mixture in terms of generalized effective Cauchy's stress tensor $\boldsymbol{\sigma}'(\boldsymbol{x}, \mathrm{t})$ [15,20] assumes the form:

$$\mathrm{div}\left(\boldsymbol{\sigma}' - \left[p^g - S_w p^c\right]\mathbf{1}\right) + \rho\mathbf{g} = 0 \tag{1}$$

where $\rho = [1\text{-}n]\rho^s + nS_w\rho^w + nS_g\rho^g$ is the mass density of the overall medium, $n(\boldsymbol{x}, t)$ is the porosity, $S_w(\boldsymbol{x}, t)$ and $S_g(\boldsymbol{x}, t)$ are respectively the water and gas degree of saturation, $\mathbf{g}$ is the gravity acceleration vector and $\mathbf{1}$ is the second order identity tensor. The form of Eq. (1) assumes the grain incompressible, which is common in soil mechanics. In order to consider compressible grains, the Biot coefficient should be present in front of the solid pressure (this becomes important when dealing with rock and concrete).

2.2 Mass balance equations

The mass conservation equation for the mixture of solid skeleton, water and its vapour is:

$$
\begin{aligned}
& n\left[\rho^{w} - \rho^{gw}\right]\left[\frac{\partial S_{w}}{\partial t}\right] + \left[\rho^{w} S_{w} + \rho^{gw}\left[1 - S_{w}\right]\right]\operatorname{div}\left(\frac{\partial \mathbf{u}}{\partial t}\right) \\
& + \left[1 - S_{w}\right] n \frac{\partial \rho^{gw}}{\partial t} - \operatorname{div}\left(\rho^{g} \frac{M_{\alpha} M_{w}}{M_{g}^{2}} \boldsymbol{D}_{\mathrm{g}}^{\mathrm{gw}} \operatorname{grad}\left(\frac{p^{gw}}{p^{g}}\right)\right) \\
& + \operatorname{div}\left(\rho^{w} \frac{\mathbf{k}^{\mathrm{w}} k^{rw}}{\mu^{w}}\left[-\operatorname{grad}(p^{g}) + \operatorname{grad}(p^{c}) + \rho^{w}\mathbf{g}\right]\right) \\
& + \operatorname{div}\left(\rho^{gw} \frac{\mathbf{k}^{\mathrm{g}} k^{rg}}{\mu^{g}}\left[-\operatorname{grad}(p^{g}) + \rho^{g}\mathbf{g}\right]\right) - \beta_{swg} \frac{\partial T}{\partial t} = 0
\end{aligned}
\tag{2}
$$

where $\mathbf{k}^{\pi}(\boldsymbol{x}, t) = k^{\pi}(\boldsymbol{x}, t)\mathbf{1}$ is the intrinsic permeability tensor of the porous matrix in π-fluid saturated condition [m^2], which is assumed to be isotropic, $k^{r\pi}(\boldsymbol{x},t)$ is the fluid relative permeability parameter and $\mu^{\pi}(\boldsymbol{x}, t)$ is the dynamic viscosity of the fluid [Pa·s], with $\pi = w, g$. $\boldsymbol{D}_{\mathrm{g}}^{\mathrm{gw}}$ is the effective diffusivity tensor of water vapour in the gas phase contained within the pore space, $\beta_{swg} = \beta_s(1-n)\cdot(S_g\, \rho^{gw} + \rho^{w} S_w)$ and M_{α}, M_w and $M_g(\boldsymbol{x},t)$ are the molar mass of dry air, liquid water and gas mixture, respectively.

Similarly, the mass balance equation for the dry air is:

$$
\begin{aligned}
& -n\rho^{g\alpha}\left[\frac{\partial S_{w}}{\partial t}\right] + \rho^{g\alpha}\left[1 - S_{w}\right]\operatorname{div}\left(\frac{\partial \mathbf{u}}{\partial t}\right) + n\left[1 - S_{w}\right]\frac{\partial \rho^{g\alpha}}{\partial t} \\
& -\operatorname{div}\left(\rho^{g} \frac{M_{\alpha} M_{w}}{M_{g}^{2}} \mathbf{D}_{\mathrm{g}}^{\mathrm{g}\alpha} \operatorname{grad}\left(\frac{p^{g\alpha}}{p^{g}}\right)\right) \\
& + \operatorname{div}\left(\rho^{g\alpha} \frac{\mathbf{k}^{\mathrm{g}} k^{rg}}{\mu^{g}}\left[-\operatorname{grad}(p^{g}) + \rho^{g}\mathbf{g}\right]\right) \\
& -\left[1 - n\right]\beta_{s}\rho^{g\alpha}\left[1 - S_{w}\right]\frac{\partial T}{\partial t} = 0
\end{aligned}
\tag{3}
$$

2.3 Enthalpy balance equation

The enthalpy balance equation of the mixture has the following form:

$$
\begin{aligned}
& \left(\rho C_{p}\right)_{eff} \frac{\partial T}{\partial \mathrm{t}} + \rho^{w} C_{p}^{w}\left[\frac{\mathbf{k}^{\mathrm{w}} k^{rw}}{\mu^{w}}\left[-\operatorname{grad}(p^{g}) + \operatorname{grad}(p^{c}) + \rho^{w}\mathbf{g}\right]\right]\cdot \operatorname{grad}T \\
& + \rho^{g} C_{p}^{g}\left[\frac{\mathbf{k}^{g} k^{rg}}{\mu^{g}}\left[-\operatorname{grad}(p^{g}) + \rho^{g}\mathbf{g}\right]\right]\cdot \operatorname{grad}T - \operatorname{div}\left(\chi_{eff} \operatorname{grad}T\right) = -\dot{\mathrm{m}}_{\mathrm{vap}}\Delta\mathrm{H}_{\mathrm{vap}}
\end{aligned}
\tag{4}
$$

where, $\rho(C_p)_{eff}$ is the effective thermal capacity of the porous medium, $C_p^w(\boldsymbol{x},t)$ and $C_p^g(\boldsymbol{x},t)$

are the specific heat of the water and gas mixture respectively, and $\chi_{eff}(\boldsymbol{x}, t)$ is the effective thermal conductivity of the porous medium. The right hand side term of Eq. (4) considers the contribution of the evaporation and condensation.

2.4 Constitutive equations

To complete the description of the mechanical behaviour, constitutive equations have to be specified. For the gas phase which is assumed to be a perfect mixture of two ideal gases, the state equation of a perfect gas (Clapeyron's equation) and Dalton's law are applied to dry air ($g\alpha$), water vapour (gw) and moist air (g). In the partially saturated zones, the water vapour pressure $p^{gw}(\boldsymbol{x}, t)$ is obtained from the Kelvin-Laplace equation. The saturation $S_\pi(\boldsymbol{x}, t)$ and the relative permeability $k^{r\pi}(\boldsymbol{x}, t)$ are experimentally determined functions of the capillary pressure p^c and the temperature T.

The behaviour of the solid skeleton is described within the framework of elasto-viscoplasticity theory for geometrically linear problems. In order to take into account the dilatant/contractant behaviour of sands, the yield function F(p', s', q) is developed in the form of Drucker-Prager for simplicity:

$$\mathrm{F}\left(p',\mathbf{s}',\mathrm{q}\right) = 3\alpha_\mathrm{F}\, p' + \left\|\mathbf{s}'\right\| - \beta_\mathrm{F}\sqrt{\frac{2}{3}}\left[\mathrm{c}_0 + \mathrm{Hq}\right] \tag{5}$$

In Eq. (5) p' = (1/3)tr$\boldsymbol{\sigma}$' is the mean effective Cauchy pressure, ||**s**'|| is the norm of the deviator effective Cauchy stress tensor $\boldsymbol{\sigma}$', c_0 is the apparent cohesion, α_F and β_F are two material parameters related to the friction angle φ of the soil defined by Eq. (6), H is the hardening/softening modulus and q is the equivalent viscoplastic strain. The flow rule is of non-associated type, with the plastic potential function given by Eq. (5) but with the dilatancy angle ψ substituting the friction angle in Eq. (6).

$$\alpha_\mathrm{F} = 2\,\frac{\sqrt{2/3}\,\sin\varphi}{3-\sin\varphi} \quad , \quad \beta_\mathrm{F} = 2\,\frac{6\cos\varphi}{3-\sin\varphi} \tag{6}$$

The viscoplastic constitutive relationships employed to model the soil behaviour are briefly outlined in the following section.

3 CONSTITUTIVE EQUATIONS FOR VISCOPLASTICITY

In viscoplasticity theory an important distinction from the inviscid plasticity theory stems from the fact that in the former the current stress states can be outside the yield surface and hence the yield function may have a value larger than zero, whereas in the latter such states are not allowed. Therefore, the Kuhn-Tucker conditions are not applicable in viscoplastic models.

The total strain rate in an elasto-viscoplastic material is additively decomposed into an elastic and a viscoplastic strain rate:

$$\dot{\boldsymbol{\varepsilon}} = \dot{\boldsymbol{\varepsilon}}^{\mathrm{e}} + \dot{\boldsymbol{\varepsilon}}^{\mathrm{vp}} \tag{7}$$

where the superimposed dot denotes time derivative. The stress rate is related to the strain rate via the following constitutive relation:

$$\dot{\boldsymbol{\sigma}} = \mathbf{D}^e : \left(\dot{\boldsymbol{\varepsilon}} - \dot{\boldsymbol{\varepsilon}}^{vp}\right) \tag{8}$$

where $\mathbf{D}^e$ is the fourth-order elastic tensor and double dots ":" denote the doubly contracted tensor product.

Two commonly used models, the Perzyna model [22] and Duvaut-Lions model [4] belong to this category. The difference between these two models is based on the different choice of the viscoplastic strain rate. Herein the first model will be treated.

In the theory proposed by Perzyna, the viscoplastic strain rate is determined by the gradient of a plastic potential function calculated at the current stress point:

$$\dot{\boldsymbol{\varepsilon}}^{vp} = \gamma \left\langle \varphi\left(\frac{F}{F_0}\right)^N \right\rangle \frac{\partial Q}{\partial \sigma'} \tag{9}$$

with F being the yield function, F_0 introduced as a reference fixed value making F/F_0 dimensionless, γ is a "fluidity" parameter which depends on the viscosity η of the material ($\gamma=1/\eta$) and can be constant or a function of the stress or strain rate, N is a calibration parameter ($N \geq 1$) and Q is the viscoplastic potential function. Associative flow is invoked by Q=F.

In above equation, "<·>" are the McCauley brackets, such that:

$$\left\langle \varphi(x) \right\rangle = \begin{cases} \varphi(x) & \text{if } \varphi(x) \geq 0 \\ 0 & \text{if } \varphi(x) < 0 \end{cases} \tag{10}$$

5 NUMERICAL EXAMPLE

In this section, the elasto-viscoplastic model presented above is applied to a plane strain compression test in case of an initially water saturated dense sand. The regularizing effect on the respective numerical simulations is discussed. The example problem was inspired by the work of [17,23]. Mesh sensitivity of the results is examined by using three different finite element discretisations. The meshes consist of 85, 340 and 1360 quadrilateral elements respectively, for a rectangular sample of homogeneous soil of 34 cm height and 10 cm width. The specimen is kept fixed horizontally and vertically at the bottom surface whereas the boundaries are impervious and adiabatic. Axial compression is applied to the specimen by imposing vertical velocity on the top nodes. Two different loading velocities were used (1.2mm/s & 0.2mm/s) to examine the influence of loading velocity on the viscous regularization of quasi-static process. Details concerning the material parameters used in the computation can be found in [23].

Figure 1 shows the contours of the equivalent viscoplastic strains in case the viscous parameter (η) is set equal to 30sec and a loading velocity (v) of 1.2 mm/sec is applied on the top surface. The mesh refinement has no influence on the width of shear band (especially for meshes with 340 and more elements) and hence the results are mesh insensitive. Mesh independency of the results is also detected from the plot of the equivalent viscoplastic strains in the vertical centre section of the sample in Figure 2(a), where proper similarity between the meshes is observable.

The importance of the considered viscous parameter and the influence of the loading velocity on the material response, are evidence through Figures 2, 3. In particular, Figure 2(b) clearly shows the dependence upon mesh refinement of both the shear band width and maximum value of viscoplastic strain, when decreasing six times the loading velocity but keep constant the viscous parameter (η = 30sec). In contrast to the mesh-dependent behaviour depicted in Figure 2(b), the results coming from the simulations with increasing viscous parameter up to 110 sec show much better characteristics (Figures 3 and 4). In these figures are presented the equivalent viscoplastic strains in the vertical centre section of the sample for the three discretisations and the corresponding contours respectively, for η=30sec and v=0.2mm/sec. No fundamental difference can be detected for results obtained by meshes with 340 or more elements.

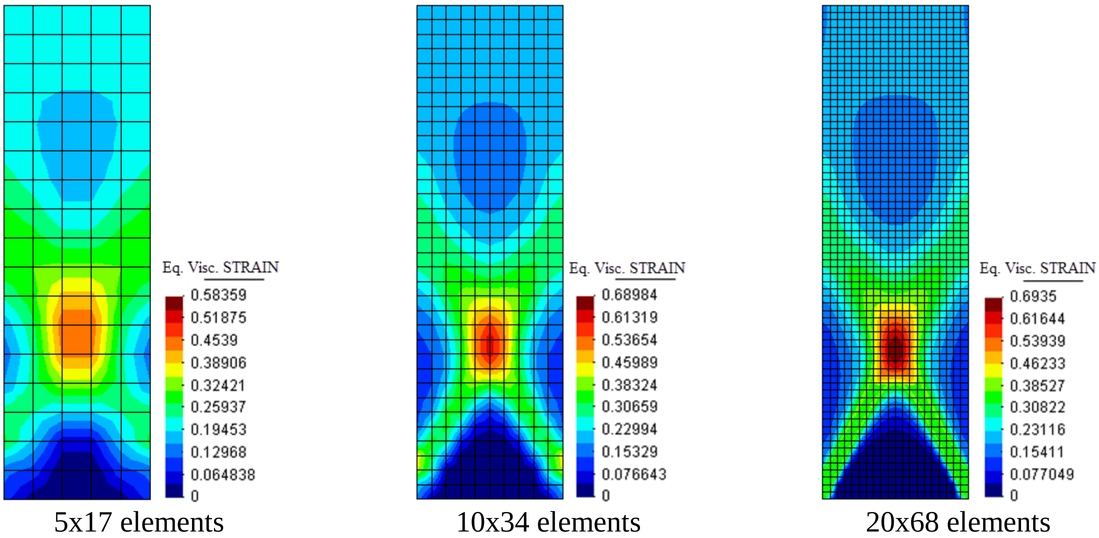

Figure 1: Equivalent viscoplastic strain contours in case v=1.2 mm/s and viscosity η=30 sec for coarse (5x17), intermediate (10x34) and fine (20x68) mesh respectively.

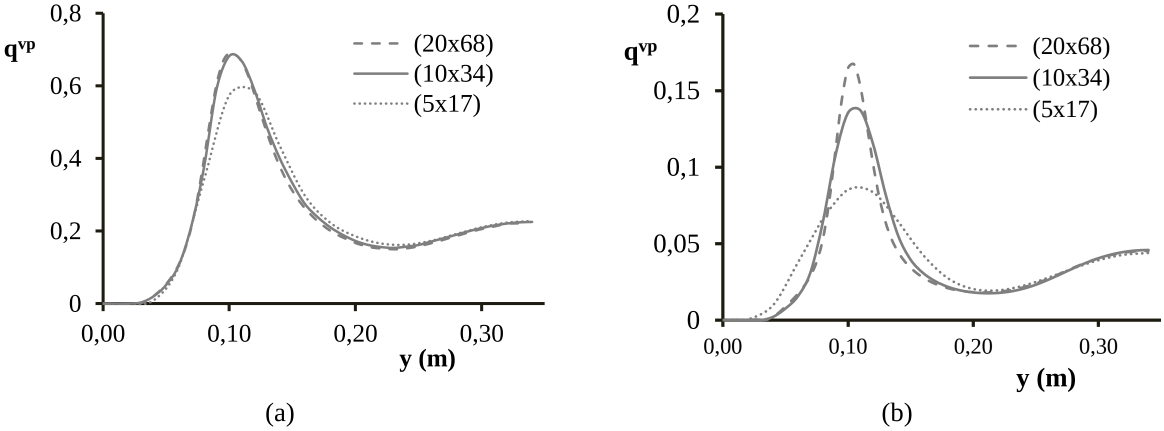

Figure 2: Distribution of the equivalent viscoplastic strains in the vertical centre section of the specimen for three meshes and viscosity η=30 sec in case (a) v=1.2 mm/s and (b) v=0.2 mm/s.

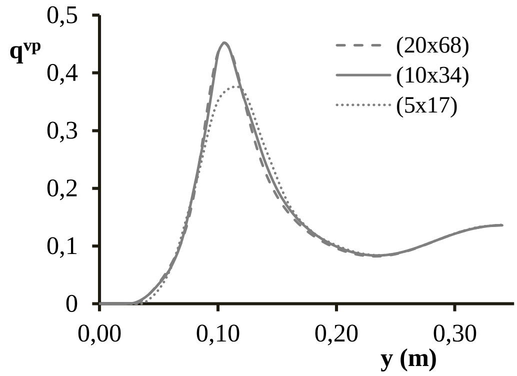

Figure 3: Distribution of the equivalent viscoplastic strains in the vertical centre section of the specimen for viscosity η=110 sec in case v=0.2 mm/s.

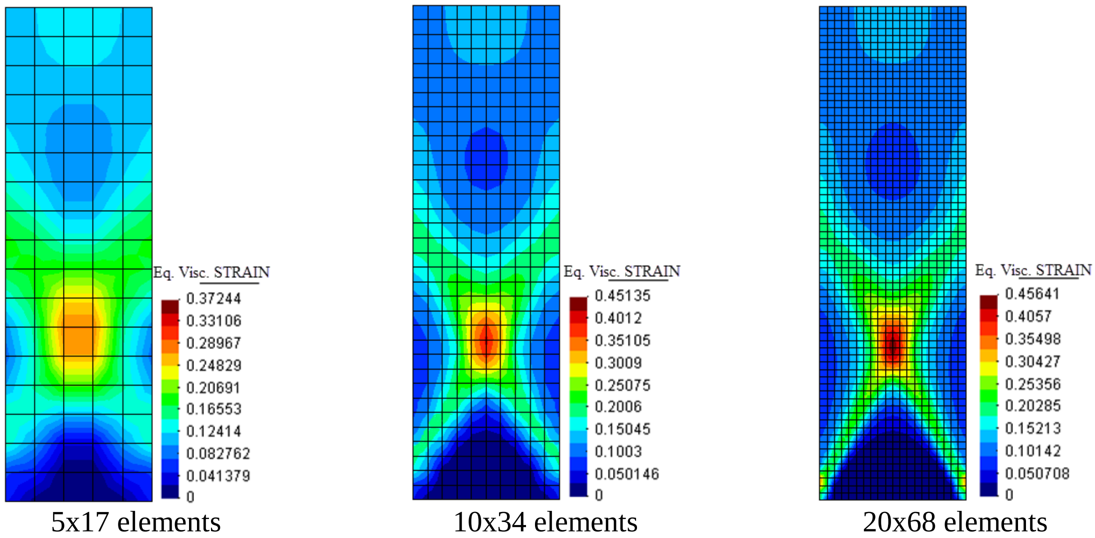

Figure 4: Equivalent viscoplastic strain contours in case v=0.2 mm/s and viscosity η=110 sec for coarse (5x17), intermediate (10x34) and fine (20x68) mesh respectively.

6 CONCLUSIONS

In the current study, the Perzyna elasto-viscoplastic model is employed to regularize the numerical solution in localization process, for the scope of mesh independency. The model is implemented in the finite element code Comes-geo developed at the University of Padua, based on the multiphase porous media model by [15]. The behaviour of the solid skeleton is described, within the framework of elasto-viscoplasticity theory, by the yield function in the form of Drucker-Prager.

Numerical results of strain localization in globally undrained dense sand have been presented for three different meshes. The results of mesh sensitivity analysis indicate that the shear band width is not exclusively governed by the viscous parameter, but depends also on the applied loading velocity. In fact, if a viscous parameter is given, for a low loading velocity the shear band width is narrow and the viscoplastic solution has mesh dependency, as the elastoplastic one. In this case, a higher loading velocity should be considered to obtain mesh independent results. In other words, for a material characterized by a specific value of viscosity the effect of loading velocity is crucial for the regularization of the numerical solution.

It should be noted that in the present work the elasto-viscoplastic model is used to obtain a regularized numerical solution and not with the aim to describe the real viscous behaviour of the soil. The behaviour of the fluids on the aforementioned plain strain localization test will be discussed in a future work.

ACKNOWLEDGMENT

The authors would like to thank the 7th Framework Programme of the European Union (ITN MuMoLaDe project 289911) for the financial support of this work.

REFERENCES

[1] Benallal, A., Berstad, T., Børvik, T. and Hopperstad, O. S. Uniqueness, loss of ellipticity and localization for the time-discretized, rate-dependent boundary value problem with softening. *Int. J. Numer. Meth. Engng* (2010) **84**:864–882.

[2] de Borst, R. Simulation of strain localization: A reappraisal of the Cosserat continuum. *Engineering Computations* (1991) **8**:317-332.

[3] di Prisco, C., Imposimato, S. and Aifantis, E.C. A visco-plastic constitutive model for granular soils modified according to non-local and gradient approaches. *International Journal for Numerical and Analytical Methods in Geomechanics* (2002), **26**:121-138.

[4] Duvaut, G. and Lions, L.J. *Inequalities in Mechanics and Physics*. Springer (1972), Berlin.

[5] Ehlers, W and Volk, W. On theoretical and numerical methods in the theory of porous media based on polar and non-polar elasto-plastic solid materials. *International Journal of Solids and Structures* (1998) **35**:4597-4617.

[6] Ehlers, W., Graf, T. and Ammann, M. Deformation and localization analysis of partially saturated soil. *Computer Methods in Applied Mechanics and Engineering* (2004) **193**:2885–2910.

[7] Gawin, D. and Schrefler, B. A. Thermo-hydro-mechanical analysis of partially saturated. *Engineering Computations* (1996) **13**(**7**):113-143.

[8] Gawin, D. and Sanavia L. A unified approach to numerical modelling of fully and partially saturated porous materials by considering air dissolved in water. *CMES-Comp. Model. Eng. Sci.* (2009) **53**:255-302.

[9] Gawin, D. and Sanavia, L. Simulation of cavitation in water saturated porous media considering effects of dissolved air. *Transport Porous Med* (2010) **81**:141-160.

[10] Gray, W.G. and Hassanizadeh, M. Unsaturated flow theory including interfacial phenomena. *Water Resour. Res.* (1991) **27**:1855-1863.

[11] Hassanizadeh, M. and Gray, W.G. General conservation equations for multi-phase system: 1. Averaging technique. *Advances in Water Resources* (1979a) **2**:131-144.

[12] Hassanizadeh, M. and Gray, W.G. General conservation Equations for multi-phase system: 2. Mass, momenta, energy and entropy equations. *Advances in Water Resources* (1979b) **2**:191-201.

[13] Hassanizadeh, M. and Gray, W.G. General conservation equations for multi-phase

systems: 3. Constitutive theory for porous media flow. *Advances in Water Resources* (1980) **3**(1):25-40.

[14] Jirásek, M. and Rolshoven, S. Comparison of integral-type nonlocal plasticity models for strain-softening materials. *International Journal of Engineering Science* (2003) **41**:1553-1602.

[15] Lewis, R.W. and Schrefler, B.A. *The Finite Element Method in the Static and Dynamic Deformation and Consolidation of Porous Media*, Wiley and Sons, Chichester, (1998).

[16] Loret, B. and Prevost, J.H. Dynamic strain localization in fluid-saturated porous media. *Journal of Engineering Mechanics* (1991) **117**(4):907-922.

[17] Mokni, M. and Desrues, J. Strain localisation measurements in undrained plane-strain biaxial tests on hostun RF sand. *Mechanics of Cohesive-Frictional Materials* (1998) **4**:419–441.

[18] Mühlhaus, H-B. and Aifantis, E.C. A variational principle for gradient plasticity. *International Journal of Solids Structures* (1991) **1**:417-438.

[19] Needleman, A. Material rate dependence and mesh sensitivity on localization problems. *Computer Methods in Applied Mechanics and Engineering* (1988) **67**:69-86.

[20] Nuth, M. and Laloui, L. Effective stress concept in unsaturated soils: Clarification and validation of a unified approach. *Int. J. Numer. Anal. Methods Geomech.* (2008) **32**: 771-801.

[21] Oka, F., Adachi, T. and Yashima, A. Instability of an elastoviscoplastic constitutive model for clay and strain localization. *Mechanics of Materials* (1994) **18**:119–129.

[22] Perzyna, P. Fundamental problems in viscoplasticity. *Advances in Applied Mechanics* (1966) **9**:243-377.

[23] Sanavia, L., Pesavento, F. and Schrefler, B.A. Finite element analysis of non-isothermal multiphase geomaterials with application to strain localization simulation. *Comput. Mech.* (2006) **37**:331-348.

[24] Sanavia, L., François, B., Bortolotto, R., Luison, L. and Laloui L. Finite element modelling of thermo-elasto-plastic water saturated porous materials. *Journal of Theoretical and Applied Mechanics* (2008) **38**: 7-24.

[25] Schrefler, B.A., Zhang, H.W. and Sanavia, L. Fluid-structure interaction in the localization of saturated porous media. ZAMM Zeitschrift für Angewandte Mathematik und Mechanik, *Journal of Applied Mathematics and Mechanics. Z. Angew. Math. Mech.* (1999) **79**: 481-484.

[26] Schrefler, B.A. Mechanics and thermodynamics of saturated/unsaturated porous materials and quantitative solutions. *Applied Mechanics Reviews* (2002) **55**(4):351-388.

[27] Schrefler, B.A., Zhang, H.W. and Sanavia, L. Interaction between different internal length scales in fully and partially saturated porous media – The 1-D case, *Int. J. for Numerical and Analytical Methods in Geomechanics* (2006) **30**: 45-70.

[28] Sluys, L.J. *Wave propagation, localization and dispersion in softening solids*, Ph.D. Dissertation (1992), Delft University of Technology.

[29] Zhang, H.W. and Schrefler, B.A. Gradient-dependent plasticity model and dynamic strain localization analysis of saturated and partially saturated porous media: one dimensional model. *European Journal of Mechanics A/Solids* (2000) **19**(3):503–524.